Chemistry and Physics of Lipids 224 (2019) 104728

Contents lists available at ScienceDirect

Chemistry and Physics of Lipids

journal homepage: www.elsevier.com/locate/chemphyslip

Cyanosomes: A pilot study

Ananya Singh[a], Farhan Ahmad[b], Priti Bajpai[a], Tarique Mahmood Ansari[c], Aisha Kamal[b,*]

[a] Department of Biosciences, Integral University, India
[b] Department of Bioengineering, Integral University, India
[c] Department of Pharmacy, Integral University, India

ARTICLE INFO

Keywords:
Cyanobacteria
Cyanosome
Liposome
Thymoquinone
Carbon tetrachloride

ABSTRACT

Cyanobacteria are the most primitive, oxygen-evolving prokaryotic organism. Several, conspicuous investigations have been done around lipids from cyanobacteria. However, to date and to the best of our knowledge, no study was conducted to formulate and evaluate liposomal vesicles prepared from cyanobacterial lipid. In the present study, cyanosomes were formulated using natural lipids extracted from the cyanobacterium *Synechococcus elongatus* PCC7942 which were further loaded with thymoquinone. The results showed that the prepared cyanosomes were homogenous with an overall negative charge of particle size ranging between 200 to 210 nm and entrapment efficacy was 70.9 ± 1.86%. The obtained release profiles demonstrated sustained drug release pattern. The study of encapsulated thymoquinone on CCl_4 induced liver insult in balb/c mice revealed the better efficacy of encapsulated thymoquinone as compared to thymoquinone alone indicating cyanosome as a promising candidate for drug carrier. However, more studies are required to establish the safety profile, pharmacokinetic pattern and biodistribution parameters of cyanosome for its clinical intricacies in future applications.

1. Introduction

Liposomes are small artificial vesicles of spherical shape that can be created from cholesterol and natural nontoxic phospholipids. Due to their size and hydrophobic and hydrophilic character (besides biocompatibility), liposomes are promising systems for drug delivery (Akbarzadeh et al.,2013). This is particularly due to the ability of liposomes to buffer the toxicity of entrapped drugs while maintaining its efficacy (Zamboni, 2005). Each drug can be loaded either in the liposomal hydrophilic core or within the lipidic bilayer and delivered eventually to the proper site into the organism. Despite, there being many marketed approved liposomal products e.g., Doxil®, Ambisome®, DepoDur™, etc., liposome based drug delivery is facing limitation as liposomal research require the use of the expensive synthetic lipids that can be procured commercially only from a handful of globally reliable suppliers. Thus, there arises a need for developing economical, biodegradable and a reliable system for preparation of liposome in order to overcome various problems.

Recently, Cyanobacteria have been recognized to posses enormous potential in serving humanity in many ways, like as biofertilizers, as human and animal feed, in bioremediation of toxic compounds, in biocontrol of pests, production of commercial and laboratory chemicals, restriction enzymes, pharmacological tools (Syiem and Bhattacharjee, 2010), also used as potential therapeutic drugs for the management of diseases like cancer, asthma, diabetes (Skulberg, 2000) and in waste and effluent water treatment including the removal of harmful dyes from textile effluents (Prassana et al., 2000; Shah et al., 2001; Sadettin and Donmez, 2007) etc. However, to date and to the best of our knowledge, no study was conducted to formulate and evaluate liposomal vesicles prepared from cyanobacterial lipid. Our particular interest in the preparation of cyanosome aroused due to the reasons that, they are easy to access all year round due to economic cultivation in various substrates, lipids and fatty acids of cyanobacterial cells helps the cell to mitigate several environmental stresses like desiccation, salt-induced damage, low temperature, high light induced photoinhibition (Singh et al., 2002). Furthermore, cyanobacterial Lipids (LPSs) have no or very less toxicity (Mohamed, 2008; Ravindranet al., 2010) in comparison to classic Gram-negative LPSs. Hence, the use of total polar lipid (TPL) from cyanobacteria appears to be a logistic approach towards development of the drug delivery vehicles thereby revolutionizing the liposome based drug delivery. Hence, the present study deals with the economical preparation of novel liposome (cyanosome) from cynobacterial lipids.

Synechococcus elongatus PCC7942 is a freshwater cyanobacteria formerly designated as *Anacystisn idulans* R2 (family *Synechococcaceae*; order *Synechococcales*) is a non-heterocystous, unicellular, obligate

* Corresponding author at: Department of Bioengineering, Integral University, Dasuli, Kursi Road, Lucknow, 226026, Uttar Pradesh, India.
E-mail address: aishakamal04@gmail.com (A. Kamal).

https://doi.org/10.1016/j.chemphyslip.2019.01.006
Received 6 June 2018; Received in revised form 19 October 2018; Accepted 16 January 2019
Available online 17 January 2019
0009-3084/

photoautotrophic microbe and its genomic sequence is available (accession number NC_007604). The objectives of this study were to formulate cyanosomes from purified TPL of cyanobacterium *Synechococcus elongatus* PCC7942 and determination of its encapsulation efficiency, morphology and drug release by entrapping thymoquinone (TQ)The study was also carried out to check its efficacy *in vivo* in CCl_4 induced liver toxicity in balb/c mice.

2. Materials and methods

2.1. Maintenance of culture

Cultures of *Synechococcus elongatus* PCC7942 were grown in the BG-11 nitrogen containing medium(KNO_3) at pH-8 and temperature 26 ± 2 °C, illuminated with white fluorescent tubes providing an intensity of 75 mol $m^{-2}s^{-1}$ and a photoperiod of 10:14 h.

2.2. Extraction and purification of lipid from Synechococcus elongatus PCC7942

The cells of cyanobacterium *Synechococcus elongatus* PCC7942 were harvested in early stationary phase for isolation of polar lipid by the method of Bligh and Dyer (Bligh and Dyer, 1959). The extracted lipid was purified on alumina oxide eluted successively with chloroform and methanol. The fraction containing total polar lipids and neutral lipids were dried under nitrogen and stored at −20 °C until further use. The purified lipids were characterized by thin-layer chromatography and employed for preparation of liposome thereby.

2.3. Preparation of cyanosomal formulation of thymoquinone

Cyanosomes were prepared by thin film hydration method. Briefly, 50 mg of lipid was used for formation of the thin film and then sonicated for 2 h in a bath-type sonicator (Qualigens) at 4 °C. The traces of undispersed lipid were removed by high-speed centrifugation. The cyanosomes formed were mixed with thymoquinone in the ratio of 5:1. The cyanosomal formulation of thymoquinone was reconstituted with phosphate buffer and pelleted by centrifugation at 14,000 rpm for 5 min followed by size reduction using probe sonicator (Labman, Chennai).

2.4. Measurement of liposome size

Transmission electron microscopy (TEM) was performed to investigate the particles size of synthesized cyanosome and thymoquinone loaded cyanosome (TQC) on an electron microscope (JEOL JEM 2100, Japan) at accelerating voltage of 200 kV. A drop of a suspension of colloidal particles was put on the carbon-coated grid and the solvent was allowed to evaporate before analysis.

2.5. Zeta-potential measurements of cyanosome and TQC

Zeta-potential was analyzed to measure the surface charge acquired by a particulate system, which defines its stability *in vitro*. The formulation was suspended in phosphate buffer (pH-7.4). The zeta-potential of dispersion was measured by the Zetasizer Nano ZS instrument (Malvern Instrument Limited, Malvern, UK). The experiment was repeated thrice.

2.6. Evaluation of the entrapment efficacy of cyanosome

The formulation, suspended in phosphate buffer (pH-7.4) was sonicated in an ultrasound bath for 15 min and then centrifuged for another 15 min at 15,000 rpm at 4^0C in a cold centrifuge. After centrifugation pellet of small unilamellar liposome (SUVs) settled at the bottom of the centrifuge tube. The supernatant was separated as it contained untrapped TQ which was soluble in chloroform and quantified by standard calibration curve prepared using TQ λ_{max} at 330 nm. The encapsulation efficiency (EE) was determined by the following equation:

EE% = (original maas of TQ in hydration solution -a mass of non-encapsulated TQ in hydration solution/ original mass of TQ in hydration solution)* 100

2.7. In Vitro drug release studies at pH 1.2 and 7.4

Once the liposome formulations was prepared, 2 ml liposome suspension was added to 10 ml of PBS (pH-7.4) followed by dissolution in HCl (pH-1.2) in 20 Eppendorf tubes. The suspension was placed into eppendorf tubes were kept in an orbital shaking water bath at 37 °C. Then, one from each set of the tubes in pH 7.4 and pH-1.2) were centrifuged for 10 min at 14,000 rpm at the interval of 0, 6, 12, 24, 48, 72, 96, 120, 140 and 160 h. To perform release kinetics studies, aliquots of supernatant were removed at different time intervals were analyzed for released TQ by measuring absorbance at 330 nm. Results obtained, were the mean values of three independent experiments.

2.8. Determination of LD_{50} of cyanosomal formulation of thymoquinone (TQC)

2.8.1. Animals

Male balb/c mice (18–22 g, 3–4 weeks old) were obtained from National Laboratory Animal Centre, Central Drug Research Institute (CDRI), Lucknow (U.P.), India and were housed in ten groups of five animals per cage for seven days prior to experimentation in an ideal laboratory environment.

2.8.2. Toxicological/safety evaluation studies of TQC in mice

Ten groups containing five male balb/c mice (18–22 g) each were used in the study. Ten doses (100–1600 mg/kg) were chosen for the determination of intraperitoneal LD_{50} in the mice. One group of mice was given 0.2 ml of olive oil intraperitoneally. Animals were weighed before the dose administration. All the animals were kept under continuous observation for any change in behavior or physical activities for 24 h after the administration of the dose.

2.8.3. Calculation of lethal dose (LD_{50})

The animals were observed for first 2 h and then at 6^{th} and 24^{th} h for any toxic symptoms. After 24 h, the number of deceased mice was counted in each group for the calculation of LD_{50}. The arithmetic method of Karber (1931) was used for the determination of LD_{50} (Ahmed, 2015).

$LD_{50} = LD_{100} – \Sigma\ (a \times b)\ n$

n = a total number of animal in a group.

a = the difference between two successive doses of administered extract/substance.

b = the average number of dead animals in two successive doses.

LD_{100} = Lethal dose causing the 100% death of all test animals.

2.9. Effect of thymoquinone loaded cyanosome against carbon tetrachloride (CCl_4) induced liver toxicity

Hepatotoxicity was induced in the male balb/c mice by administration of CCl_4 intraperitoneally (Nagiet al., 1999).The mice were randomly divided into following groups consisting of five animals each (n = 5).

Group I: control (C): Injected with saline water at a dose of 0.2 ml/20 g animal i.p.

Group II: Toxic (TC) group: Injected with CCl_4 at a dose 20 µl/Kg, i.p. in olive oil [10].

Group III: Thymoquinone (TQ) group: Injected with thymoquinone at LD_{50} dose i.e. 90.3 mg/kg (Mansour et al., 2001), one hour prior to CCl_4 intoxication.

Group IV: Thymoquinone loaded cyanosome (TQC) group: Injected at LD_{50} dose i.e, 400 mg/kg (liposome to drug ratio 5:1) one hour before CCl_4 intoxication.

2.9.1. Blood sampling from mice

The blood from all the groups was collected from retro-orbital plexus with a sterile capillary tube and collected in EDTA vacutainer tubes. The liver tissues were collected after euthanizing the animals with thiopental sodium. All the procedures were performed as per the guidelines of Committee for the Purpose of Control and Supervision of Experiments on Animals (CPCSEA).

2.9.2. Estimation of liver enzymes

Estimation of serum levels of alanine transaminase (ALT, EC:2.6.1.2), aspartate transaminase (AST, EC:2.6.1.1) were measured by standard protocols. Total bilirubin was also measured using the semi-auto analyzer.

2.9.3. Preparation of liver tissue homogenate

10% (w/v) homogenate of mice liver was prepared with the aid of York's homogenizer fitted with Teflon plunger in 0.1 M phosphate buffer (pH 7.4). The whole homogenate was first centrifuged at 100,000 rpm for 10 min. The pellet consisting of nuclear fraction and cell debris was discarded. The supernatant was further centrifuged at 11,000 rpm for 15 min and the mitochondrial fraction was separated. The clear supernatant was further centrifuged at 100,000 rpm for 30 min and the resulted supernatant was used for enzyme activities.

2.9.4. Determination of lipid peroxide level

Lipid peroxide level was measured by Ohkawa et al. (1979). Briefly, 0.2 ml of each sub-cellular fraction having 3–10 mg protein, was mixed with 1.0 ml of 20% acetic acid followed by the addition of 0.2 ml of 8% aqueous SDS. The mixture was adjusted to pH-4, 1.5 ml of 0.8% TBA solution and sufficient amount of distilled water was also added to achieve the final volume to 4 ml. The reaction mixture was incubated in a boiling water bath for an hour. After cooling to room temperature, 3 ml of n-butanol was added. The reaction mixture was centrifuged at 10,000 rpm for 15 min A clear butanol fraction obtained by centrifugation was used for measuring the absorbance at 532 nm.

2.9.5. Determination of antioxidant enzymes activities

2.9.5.1. Estimation of superoxide dismutase activity. The superoxide dismutase assay was performed by the method of Gianopolitis and Ries (1977). The reaction mixture comprised of 0.002 mM riboflavin, 13 mM methionine, 0.025 mM nitrobluetetrazolium (NBT), 50 mM sodium carbonate (pH 10.2), and the appropriate volume of extract. Distilled H_2O was added to bring final volume to 3 ml. The mixtures were illuminated for 15 min in glass test tubes. Identical solution that was not illuminated served as blank. Absorbance was measured at 560 nm. The unit of enzyme activity is defined as the amount of enzyme required to inhibit the reduction in optical density of NBT up to 50%, in 1 min at 560 nm under the assay condition. Results were expressed as unit/mg protein.

2.9.5.2. Estimation of catalase activity. Catalase activity was determined by the method of Aebi (1974) with minor modification. Briefly, the activity was determined by measuring the decrease in absorbance at 240 nm of a reaction mixture consisting of H_2O_2, in phosphate buffer, pH 7.0, and requisite volume of tissue supernatant (cytosolic fraction). The molar extinction coefficient of 43.6Mcm^{-1} was used to determine catalase activity. The specific activity was calculated and was expressed as unit/min/mg of total protein.

2.9.6. Determination of reduced glutathione (GSH) content

The reduced glutathione was determined by Eliman (2019). Briefly, 1 ml liver homogenate (10%) was deproteinized by adding 1 ml of 10% TCA and centrifuged at 10,000 rpm for 5 min. 0.5 ml aliquots of the supernatant mixed with 0.5 ml of double distilled water thereafter 2 ml of 0.4 M Tris buffer and 0.1 ml 5, 5′-dithio bis 2-nitrobenzoic acid (DTNB) were added to it with proper stirring. The absorbance was recorded at 412 nm within 5 min of the addition of DTNB.

2.9.7. Histopathological examination of liver sections

Different specimens were obtained from the liver of each mouse. Specimens were fixed in 10% neutral buffered formalin for 24–48 h, dehydrated in graded alcohol series, cleared in xylene and embedded in paraffin wax. Paraffin-fixed specimens were cut at 4 μm tissue sections. The sections (one section/each specimen) were stained with hematoxylin and eosin stain (H and E stain). The stained sections were examined under a light microscope (Olympus CX31, Japan) and photographed using a digital camera (Olympus, Camedia-5060, Japan). The most common pathological findings were recorded.

2.9.8. White blood cell counts

20 ml of blood was used to determine total WBC counts. WBC counts were measured with a microcell counter. 3 ml of blood was smeared onto a microscope glass and after staining with MayGrunnwald-Giemsa according to standard procedures, percentages of granulocytes and lymphocytes were counted.

2.9.9. Immunological studies

Interferon factors-gamma (IFN-γ), tumor necrosis factor (TNF-α) and Interleukin–2 (IL–2) levels were determined by sandwich ELISA on sera of all groups according to manufacturer instructions.

2.10. Statistical analysis

Statistical analysis was performed as the mean ± SD followed by one way ANOVA test using Graph Pad Prism and for multiple comparison tests among the groups, Tukey's test was performed. The significant level was set at $p < 0.05$.

3. Results

3.1. Liposome formulation (drug to lipid ratio)

In many studies drug-lipid interactions have been observed (Xu et al., 2011, 2012; Sylvester et al., 2016) which may affect loading efficiency. The appropriate D/L ratio can regulate the presence and the intensity of these interactions, so that an optimal formulation is achieved. The D/L ratio may be used to determine the number of doses required to achieve the therapeutic one. Taking into consideration, a number of sequels of liposome suspensions were prepared, with different contents of lipids and thymoquinone, dispersed in phosphate buffer (pH 7.4). In this sequel, the D/L ratio was optimized to obtain the maximum entrapment efficiency with desired shape and size. The different drug to lipid ratio endeavored during optimization was summarized in Table 1. In the series of trials, the best encapsulation capacity of thymoquinone in cyanosome was found to be in Trial#1, but the size of liposome was found to be very large during microscopic examination. However, Trial#2 was found to be the more suitable sequel for thymoquinone encapsulation inside cyanosome in terms of

Table 1
Drug to lipid ratio optimization.

Trial#	Drug (mg)	Lipid (mg)	Encapsulation efficiency (%)
1	5	50	75 ± 1.50
2	10	50	70 ± 1.25
3	20	50	60 ± 2.25
4	30	50	40 ± 1.95
5	40	50	35 ± 3.20

both entrapment efficiency and desired shape and size.

3.2. Drug entrapment efficiency of thymoquinone loaded cyanosome (TQC)

Drug entrapment efficiency of TQC was determined spectrophotometrically at 330 nm (Systronics 2020). A standard graph was plotted with 1–7 mg/ml of thymoquinone dissolved in chloroform. The entrapment efficiency of TQ in TQC was found to be 70.9 ± 1.86%. However, in another studies, the encapsulation efficacy of TQ was determined to be 62% in thymoquinone-loaded PLGA nanoparticles (Nallamuthu et al., 2013), ~91% entrapment efficiency was found in thymoquinone loaded liposome (Khan et al., 2015). Likewise, in another report two types of liposomes were prepared, DPPC liposomes (LP) and DPPC-Triton X-100 liposomes (XLP). In these studies entrapment efficiency of thymoquinone-loaded liposomes (TQ-LP) was found to be more than 90% and 49.6% for thymoquinone loaded in liposomes modified with Triton X-100 (XLP) (Odeh et al., 2012). Therefore, the present novel preparation of thymoquinone loaded cyanosome showed quite appreciable encapsulation efficiency which might enhance its bioavailability as well as biomedical application.

3.3. Physicochemical characterization of cyanosome and TQC

The functional utility of liposome-based drug delivery systems depends on the physicochemical nature of the nanoparticles, such as size, morphology, charge, and physical state. The polydispersity index (PdI) of free and thymoquinone loaded cyanosome was found to be 0.472 and 0.424 respectively. The diffusion light scattering results showed that the size of cyanosome and thymoquinone loaded cyanosome were 206 nm and 210 nm respectively. Further, zeta potential was −48.0 and −49.4 for the cyanosome and TQC respectively which indicated negatively charged surface and stable nano-formulations. TEM analysis confirmed that the particles were discreetly spherical in shape with mono-dispersed size distribution for both the cyanosome and TQC (Fig.1). However, in the present study, the liposome size was found to be more when observed by DLS as compared to the TEM. Similar variable results were also observed by Wang et al. (2010) and they explained that the variation in size may be due to the reason that the size measured by DLS is related to the hydrodynamic diameter while TEM results are related to the dry state.

3.4. In vitro drug release kinetics

The drug release kinetics showed sustained release of thymoquinone from cyanosome at a physiological pH of 7.4 in phosphate buffer and within 6 h, it was found to be 6% which was gradually increased with the time period. After 160 h approximately 68% of TQ was released from cyanosome (Fig.2A). The drug present at or just beneath the surface of the cyanosome is responsible for the burst release followed by sustained release of the drug from the nanoparticle core. However, at pH-1.2 it was found that cyanosome was releasing the higher amount of TQ. After 160 hit was found to be 85% which was 17% greater than drug released at alkaline pH-7.4 (Fig.2B). There was more pronounced sustained drug release at acidic pH as compared to alkaline pH which favored intraperitoneally delivery of formulation. Further, the release kinetics revealed the slow and sustained release of drug from the thymoquinone loaded cyanosomes (TQC). The pH-sensitive property of drug release from cyanosome might be beneficial for combating side effects of liposomes in circulation by reducing release rate at neutral pH and enhancing specific release in various benign and malignant upper gastrointestinal diseases which usually possess very low acidic pH (Lu et al., 2010).

3.5. Determination of LD_{50} of thymoquinone loaded cyanosome (TQC)

Two hours post-treatment, animals in each group were examined for any abnormal symptoms and determining the lethal dose of thymoquinone loaded cyanosome. No abnormalities were observed at the doses ranging from 100 to 400 mg/kg, however, at the dose of 600 mg/kg and 800 mg/kg water intake of mice was increased. With an increase in dose from 1000 to 1600 mg/kg, dizziness and irritation were also observed along with increased water intake and less responsiveness. The severity of these effects was related to the level of dose. After 24 h, the number of deceased mice was counted in each group (Table 2). The LD_{50} was found to be 400 mg/kg i.p.

3.6. Effect of TQ and TQC treatment on SOD, CAT, lipid peroxidation and reduced glutathione (GSH) level in liver tissue

The present study clearly asservate the antioxidant potential of thymoquinone and its formulation in combating oxidative stress by

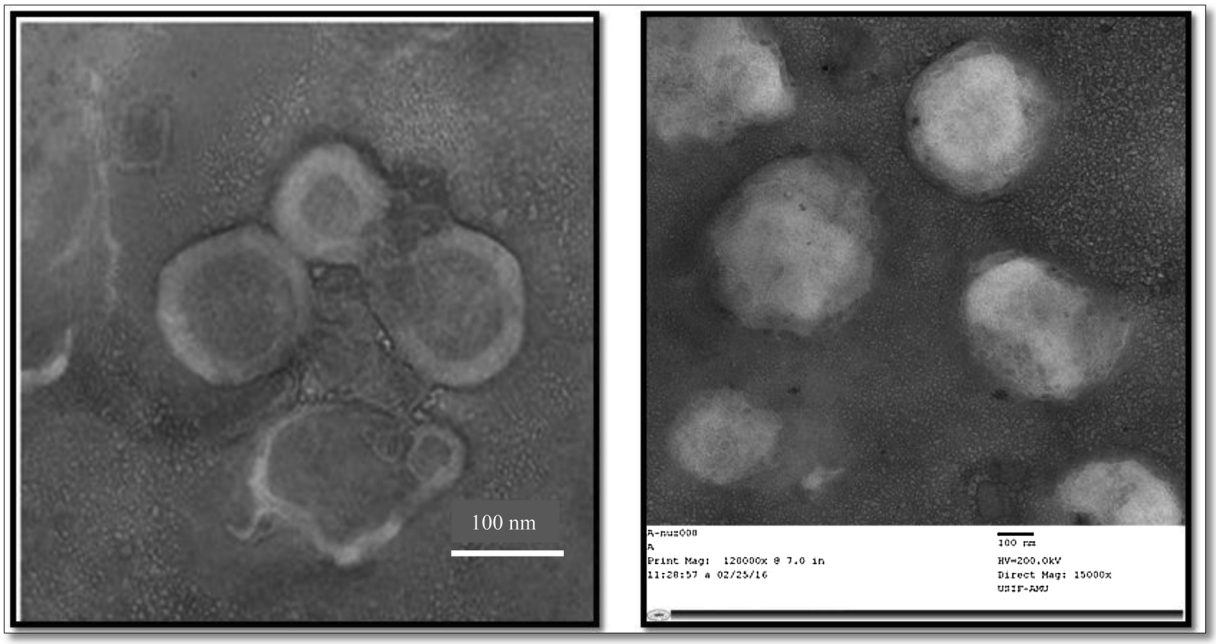

Fig. 1. TEM image of TQ encapsulated cyanosomes. The average diameter of liposomes is about 100 nm.

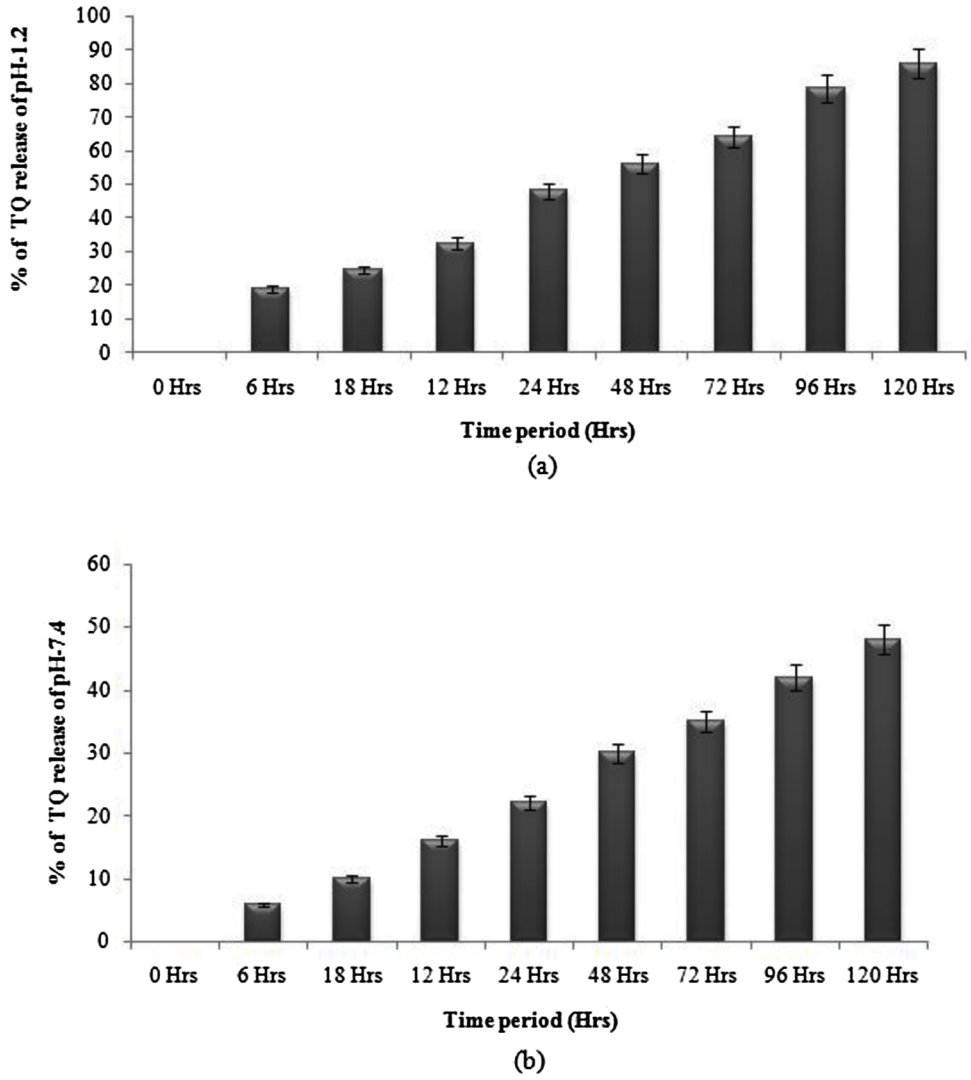

Fig. 2. Drug release from cyanosome (A) In vitro release of TQ from TQ-loaded cyanosome in PBS (0.01 M, pH = 1.2), (B) in vitro release of thymoquinone from TQ-loaded cyanosome in PBS (0.01 M, pH = 7.4). All the values are expressed as mean ± SD (n = 3).

restoration of the activity of antioxidant SOD, CAT and GSH; instigated by administration of CCl_4. In the current study activities of both SOD and CAT was significantly decreased in the toxic group after CCl_4 administration (5.54 ± 0.293and 2.17 ± 0.232 unit/mg of protein respectively) as compared to the control (11.75 ± 0.499 and 5.04 ± 0.002unit/mg of protein respectively) whereas pretreatment of the CCl_4 treated group with TQ and TQC showed a significant rise in the activity of antioxidant enzymes SOD and CAT (Fig. 3A & B). The CCl_4 treatment caused a considerable increase in liver malondialdehyde (MDA) content to 5.23 ± 0.417nmoles/mg with concomitant significant fall in the liver GSH content 0.55 ± 0.582μM/mg in the toxic group as compared to control group (Fig. 4A& Fig. 4B). Pretreatment with TQ before CCl_4 administration demonstrated a significant decrease in liver MDA content 4.53 ± 0.358 nmoles/mg and an increase in the GSH content 5.282 ± 0.11μM/mg. In contrary to TQ, pretreatment with TQC before CCl_4 dispensation leads to a more significant decrease in MDA content (3.84 ± 0.182 nmoles/mg) with an eloquent increase in liver GSH content (4.51 ± 0.171 μM/mg) (Fig. 4A & B).Interestingly in all the above study pretreatment with TQC was found more pronounced as compared to TQ alone. Our results are

Table 2
Toxicological/safety evaluation studies in mice.

S.NO.	Group	Dose	Mortality(x/n)	Symptoms after 2 hrs.
1	Group I	Vehicle	0	Nil
2	Group II	100(mg/kg)	0	Nil
3	Group III	200(mg/kg)	0	Nil
4	Group IV	400(mg/kg)	0	Nil
5	Group V	600(mg/kg)	0	Water intake increased
6	Group VI	800(mg/kg)	1	Water intake increased
7	Group VII	1000(mg/kg)	2	Dizziness, water intake increased
8	Group VIII	1200(mg/kg)	2	Dizziness, irritation, water intake increased
9	Group IX	1400(mg/kg)	3	Dizziness, irritation, water intake increased
10	Group X	1600(mg/kg)	4	Dizziness, irritation, water intake increased

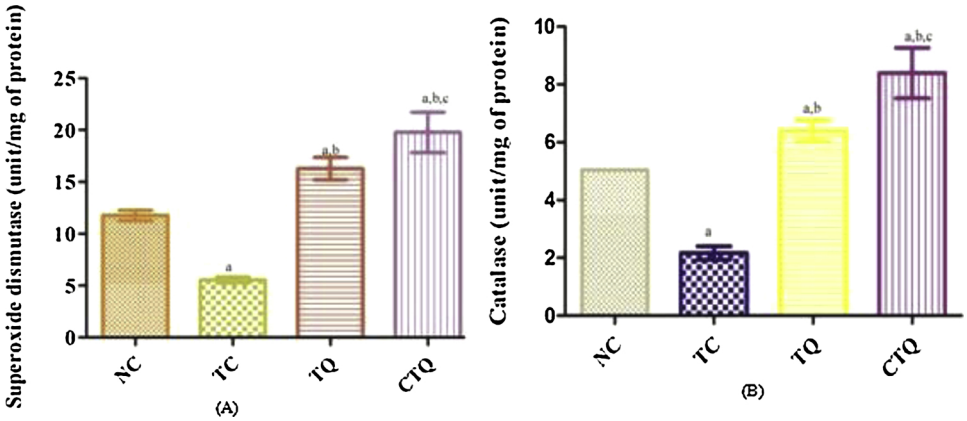

Fig. 3. Effect of thymoquinone (TQ) and thymoquinone loaded cyanosome (TQC) treatment on the level of liver enzyme (A) SOD (B) CAT in CCl_4 induced liver toxicity in male balb/c mice. Data represent the mean ± SD (*p < 0.05 significance to normal control *a, significance to toxic control *b and significance to thymoquinone treated group *c. Post-hoc Tukey's test was performed to analyze the results which were different from the others.

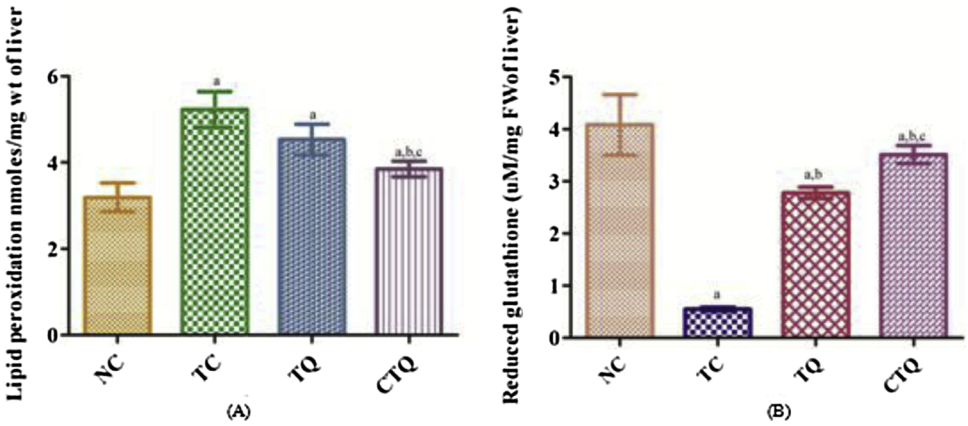

Fig. 4. (A) Effect CCl_4, TQ and TQC on the level of reduced glutathione (B) Effect CCl_4, TQ and TQC on the level of lipid peroxidation. Data represent the mean ± SEM (*p < 0.05 significance to normal control *a, significance to toxic control *b and significance to thymoquinone treated group *c. Post-hoc Tukey's test was performed to analyze the results which were different from the others.

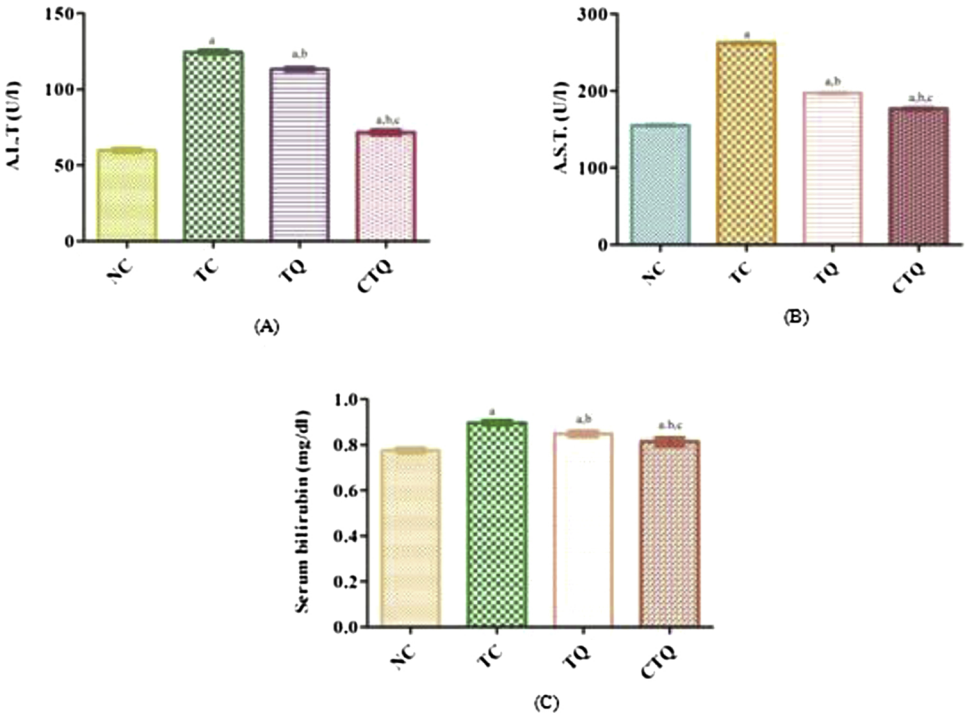

Fig. 5. (A) Effect CCl_4, TQ and TQC on the level of liver enzymes of A.L.T (B) A.S.T and (C) serum bilirubin. Data represent the mean ± SEM (*p < 0.05 significance to normal control *a, significance to toxic control *b and significance to thymoquinone treated group *c. Post-hoc Tukey's test was performed to analyze the results which were different from the others.

also in the agreement with several other studies demonstrating the antioxidant and hepatoprotective effects of thymoquinone against CCl_4-induced hepatotoxicity in isolated rat hepatocytes (Badary et al., 2003; El-Tawil and Moussa, 2006; El-Sayed, 2011; Essawy et al., 2012; Laskar et al., 2016).

3.7. Effect of TQ and TQC treatment on liver enzymes (ALT & AST) and serum bilirubin

CCl_4 intoxication resulted in oxidative stress that led to the lesion in the liver along with changes in the liver marker enzymes, biochemical

Table 3
Effect CCl_4, TQ and TQC on WBCs, % of lymphocytes and % of granulocytes of mice injected with CCl_4.

Groups	WBCs (10^3/ml)	% of lymphocytes	% of granulocytes
Control	4.63 ± 1	65.5 ± 2.45	10.26 ± 1.58
CCl_4	7.83 ± 2.12	48 ± 1.95	18.95 ± 1.54
TQ	5.88 ± 1.45	58 ± 1.25	14.21 ± 1.35
TQC	5.25 ± 1.50	62 ± 2.85	11.23 ± 2.25

markers and antioxidant defense enzymes. The results obtained with CCl_4 treatment and changes induced with TQ and TQC on liver function tests depicted in Fig. 5A and B. Compared to the control group, the levels of serum alanine aminotransferase (ALT) and aspartate transaminase (AST) in the toxic control group were increased from 58.8 to 124.4U/l and 155.2 to 262.0U/l respectively. While treatment with TQ (TQ group) the level of ALT and AST significantly reduced to 113.2 ± 1.304 U/l and 197.0 ± 0.707 U/l. Moreover, TQC reduced the level of ALT and AST 71.60 ± 1.673 U/l and 176.6 ± 1.342 U/l respectively and found to be more compelling as compared to free TQ in ameliorating the CCl_4 induced elevation of ALT and AST (Fig. 5A& B). The level of serum bilirubin had also been increased in the CCl_4 group as compared to control by 15.46%. Moreover, pretreatment of mice with TQ and TQC significantly suppressed the level of serum bilirubin by 5.35% and 9.15% respectively (Fig. 5C).Previous reports showed that the increased level of serum ALT and AST induced by CCl_4 found to be the major reason for cell membrane and liver mitochondrial damage (Mehmetçik et al., 2008; Arici and Çetin, 2011). The comparative analysis of LD_{50} dose of TQ (90.3 mg/kg) and TQC (400 mg/kg) had shown that pretreatment of mice withTQ alone and TQC significantly ameliorated the effects of CCl_4 induced hepatotoxicity evidenced by the decreased level of liver enzymes. The mitigation of increased level of serum enzymes in CCl_4-induced liver damage by TQ and TQC may be due to the prevention of the leakage of intracellular enzymes by its membrane stabilizing activity due to the healing of hepatic parenchyma and the regeneration of hepatocytes.

3.8. White blood cell count

The results showed increased WBCs count and the percentage of granulocytes in CCl_4 group as compared to the control group. On the other hand, the percentage of lymphocytes was declined in CCl_4 group as compared to control group (Table 3). However, pretreatment of CCl_4 challenged mice with TQ and TQC, led to the decline of WBCs count and percent of granulocytes. Interestingly, in all the cases pretreatment with TQC had shown the more pronounced result as compared to the TQ alone (Table 3). In present study, intraperitonial injection of balb/c mice with CCl_4 had shown the reduced percentage of lymphocytes population in the blood which is among one of the indications of the decline of immune activity by liver damage. In contrary CCl_4 challenge led to the increased number of WBCs count which may be attributed to the defensive mechanism of the immune system (Patrick-Iwuanyanwu et al., 2007). The ability of CCl_4 to increase WBCs count indicates that it can influence the defense mechanism of injected mice and mediate inflammation (Oluyemi et al., 2007).

3.9. Inflammatory cytokines

The study showed a significant increase in the mean of TNF-α (256.5 ± 2.121 pg/ml) and IFN-γ (75.5 ± 0.707 pg/ml) of CCl_4 group compared to the mean of TNF-α (50.38 ± 0.728 pg/ml) and IFN-γ(40.48 ± 0.671 pg/ml) of the normal group. However, there was a significant decrease in the mean of IL-2 of CCl_4 group (15.50 ± 0.707 pg/ml) when compared with the normal group (23.83 ± 0.247 pg/ml). Pretreatment of CCl_4 challenged mice with TQ and TQC led to the significant decline in the level of the TNF-α and IFN-γ when compared with a CCl_4 group (Fig.6A &B). On the other hand, pretreatment with TQC and TQ led the decrease in the mean of IL-2

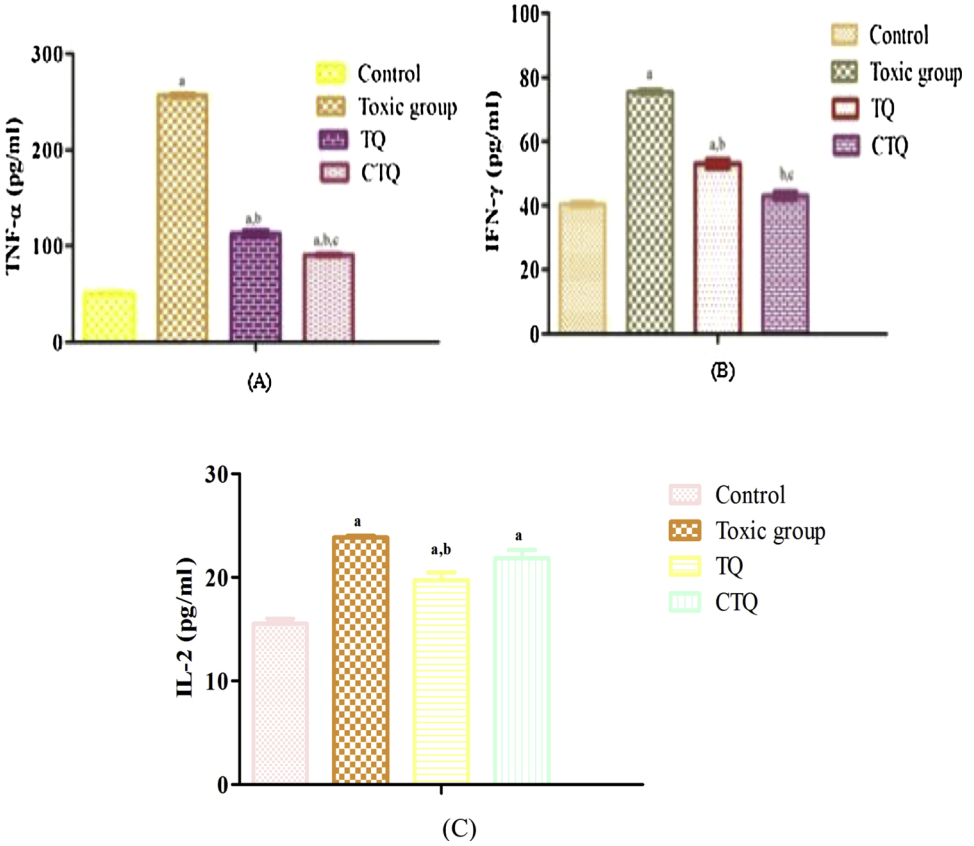

Fig. 6. (A) Effect CCl_4, TQ and TQC on the level of liver enzymes of (A) TNF-α (B) IFN-γ (C) IL-2 Data represent the mean ± SEM (*$p < 0.05$ significance to normal control *a, significance to toxic control *b and significance to thymoquinone treated group *c. Post-hoc Tukey's test was performed to analyze the results which were different from the others.

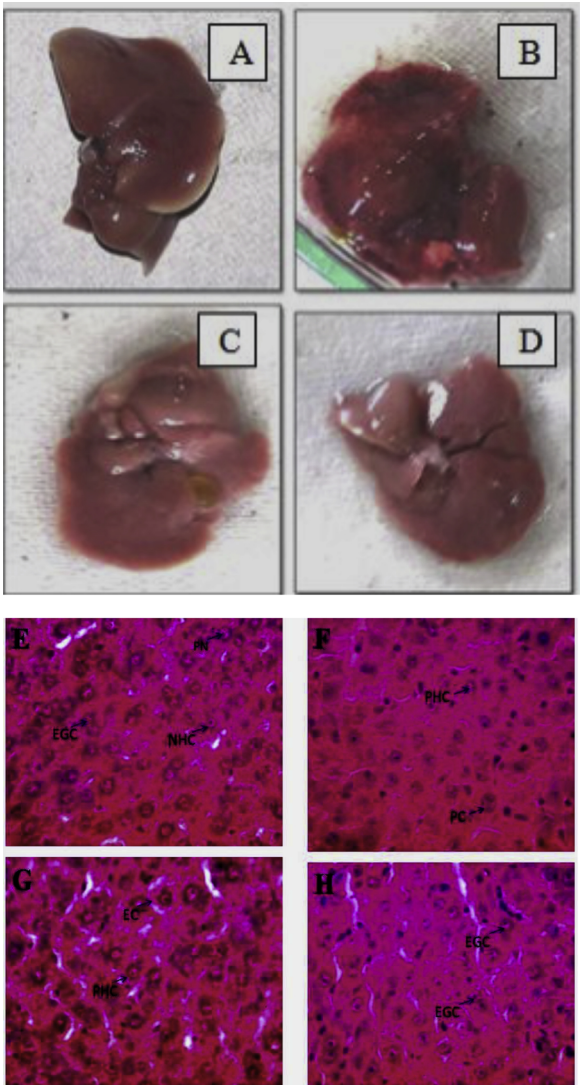

Fig. 7. Intact liver of (A) control (B) TC group (C) TQ group (D) TQC group and hematoxylin and eosin-stained sections of male balb/c mice liver (E) control (F) TC group (G) TQ group (H) TQC group.

compared to CCl_4 group (Fig. 6C). In consistence with the increased number of WBCs, the levels of TNF-α and IFN-γ were increased after injection of balb/c mice with CCl_4. TNF-?? is a pro-inflammatory cytokine that is elevated in acute and chronic diseases and stimulates the release of cytokines from macrophages and induces phagocyte oxidative metabolism (Schwabe and Brenner, 2006). The results further demonstrated that the pretreatment of CCl_4 challenged mice with TQ and TQC led to the reduction in the evel of TNF-α and IFN-γ demonstrating the anti-inflammatory activity of TQ and TQC respectively. IL-2 characterized as a pro-inflammatory cytokine that is secreted by Th1 cells. IL-2 plays a central role in the activation of regulatory T cells to produce the cytokines TNF-α and IFN-γ (Fridman et al., 2012). The declined level of the mean of IL-2 compared with CCl_4 group after pretreatment with TQC and TQ also supports the anti-inflammatory response of TQ. The downsizing of IL-2 might lead to the down regulation of TNF-α and IFN-γ in addition to the anti-inflammatory response of TQ.

3.10. Histological examinations of liver sections

Hematoxylin and eosin stained liver sections from control mice revealed normal hepatocytes (NHC) with well-preserved cytoplasm, prominent nucleus (PN), nucleolus, central vein and compact arrangement of hepatocytes with abundant eosinophilic granular cytoplasm (EGC) with distinct cell boundaries. Hepatocytes are separated by sinusoids containing Kupffer cells and arranged in trabecules running radiantly from the central vein. Hepatocytes are regular and contain a sizeable spheroidal nucleus with a distinctly marked nucleolus and peripheral chromatin distribution (Fig. 7E). In contrast, CCl_4 resulted in liver injury (Fig. 7B) and the caused proliferated hepatocytes (PHC) with an increased intercellular space with few nuclei showing pyknotic changes (PC) with condensed chromatin, lack of nucleolus and strongly acidophilic cytoplasm were also observed. Vascularity has also been changed (Fig. 7F). The cytoplasm of hepatocytes contained empty vacuole-like spaces, and the central vein was dilated and congested with a solid focal collection of inflammatory cells in the necrotic parenchyma. Few hepatocytes with necrotic features were also observed. However, TQ treated mice exhibited proliferated hepatocytes (PHC) with normal and abundant eosinophilic cytoplasm (EC) with distinct cell boundaries. The architecture was found to be maintained with increased interstitial cells and increased vascularity (Fig. 7G). Moreover, pretreatment with TQC before CCl_4 administration significantly ameliorated the liver histological lesion and maintained normal hepatocytes with abundant eosinophilic granular cytoplasm (EGC) with distinct cell boundaries. (Fig. 7H).Central veins were separated by sinusoids containing Kupffer cells, and the trabecular structures of liver were restored. Cytoplasm showed a clear visualization without any blurred appearance. The architecture was found to be more maintained with increased interstitial cells and increased vascularity as compared to TQ alone. The biochemical studies were thus supported by histopathological observation in confirming the better efficacy of TQC in withstanding the adversity of CCl_4 intoxication which could be attributed to the enhanced bioavailability and sustained drug release from the cyanosome at the affected site.

4. Conclusion

To the best of our knowledge, the present study is the first report on using cyanobacterial lipid as a toolbox for the successful biodegradable and biocompatible preparation of liposome. Importantly, the use of natural lipids from cyanobacteria will circumvent the need for the costly synthetic lipid for the preparation of liposome. In the study experimental conditions, such as the concentration of lipid to drug ratio, sustained release behavior and solution pH has been optimized to engineer cyanosome, a novel drug carrier. However, more studies are required to establish the safety profile, pharmacokinetic pattern and biodistribution parameters of cyanosome for its clinical intricacies in future applications, however, the above data indicate an important new delivery gateway for delivery of various drugs and hold the promise of a safe and efficacious delivery vehicle from natural lipids.

Authors' contributions

All authors equally participated in designing of experiments, acquisition of results, statistical analysis and drafting of the manuscript. All authors read and approved the final manuscript.

Funding

This research did not receive any specific grant from funding agencies in the public, commercial, or not-for-profit sectors.

Conflict of interest

The authors declare that they have no competing interests.

Acknowledgment

The authors greatly endorse National Laboratory Animal Centre, Central Drug Research Institute (CDRI), Lucknow (U.P.) for providing animals and their keen guidance and support in nurturing and upkeeping of animals.

References

Aebi, H., 1974. Catalase. In: Bergmeyer, U. (Ed.), Methods of Enzymatic Analysis.
Ahmed, M., 2015. Acute toxicity (Lethal Dose 50 Calculation) of herbal drug Somina in rats and mice. Pharmacol. Pharm. 6 (03), 185.
Akbarzadeh, A., Rezaei-Sadabady, R., Davaran, S., Joo, S.W., Zarghami, N., Hanifehpour, Y., Samiei, M., Kouhi, M., Nejati-Koshki, K., 2013. Liposome: classification, preparation, and applications. Nanoscale Res. Lett. 8 (1), 102.
Arici, O.F., Çetin, N., 2011. Protective role of ghrelin against carbon tetrachloride (CCl_4)-induced coagulation disturbances in rats. Regul. Pept. 166 (1), 139–142.
Badary, O.A., Taha, R.A., Gamal El-Din, A.M., Abdel-Wahab, M.H., 2003. Thymoquinone is a potent superoxide anion scavenger. Drug Chem. Toxicol. 26 (2), 87–98.
Bligh, E.G., Dyer, W.J., 1959. A rapid method of total lipid extraction and purification. Can. J. Biochem. Physiol. 37 (8), 911–917.
Eliman, G.L., 2019. Tissue sulfhydryl group. Arch. Biochem. Biophy 82, 70–77.
El-Sayed, W.M., 2011. Upregulation of chemoprotective enzymes and glutathione by Nigella sativa (black seed) and thymoquinone in CCl4-intoxicated rats. Int. J. Toxicol. 30 (6), 707–714.
El-Tawil, O., Moussa, S.Z., 2006. Antioxidant and hepatoprotective effects of thymoquinone against carbon tetrachloride-induced hepatotoxicity in isolated rat hepatocyte. J. Egypt Soc. Toxicol. 34, 33–41.
Essawy, A.E., Abdel-Moneim, A.M., Khayyat, L.I., Elzergy, A.A., 2012. Nigella Sativa Seeds Protect Against Hepatotoxicity and Dyslipidemia Induced by Carbon Tetrachloride in Mice.
Fridman, W.H., Pagès, F., Sautès-Fridman, C., Galon, J., 2012. The immune contexture in human tumours: impact on clinical outcome. Nat. Reviews Cancer. 12 (4) p.nrc3245.
Khan, M.A., Aljarbou, A.N., Khan, A., Younus, H., 2015. Liposomal thymoquinone effectively combats fluconazole-resistant Candida albicans in a murine model. Int. J. Biol. Macromol. 76, 203–208.
Laskar, A.A., Khan, M.A., Rahmani, A.H., Sana, F., Younus, H., 2016. Thymoquinone, an active constituent of Nigella sativa seeds, binds with bilirubin and protects mice from hyperbilirubinemia and cyclophosphamide-induced hepatotoxicity. Biochimie. 127, 205–213.
Lu, P.J., Hsu, P.I., Chen, C.H., Hsiao, M., Chang, W.C., Tseng, H.H., Lin, K.K., Chuah, S.K., Chen, H.C., 2010. Gastric juice acidity in upper gastrointestinal diseases. World J. Gastroenterol. 16 (43), 5496.
Mansour, M.A., Ginawi, O.T., El-Hadiyah, T., El-Khatib, A.S., Al-Shabanah, O.A., Al-Sawaf, H.A., 2001. Effects of volatile oil constituents of Nigella sativa on carbon tetrachloride-induced hepatotoxicity in mice: evidence for antioxidant effects of thymoquinone. Res. Com. Mol. Pathol. Pharmacol. 110 (3-4), 239–252.
Mehmetçik, G., Özdemirler, G., Koçak-Toker, N., Çevikbaş, U., Uysal, M., 2008. Role of carnosine in preventing thioacetamide-induced liver injury in the rat. Peptides. 29 (3), 425–429.
Mohamed, Z.A., 2008. Toxic cyanobacteria and cyanotoxins in public hot springs in Saudi Arabia. Toxicon. 51 (1), 17–27.
Nallamuthu, I., Parthasarathi, A., Khanum, F., 2013. Thymoquinone-loaded PLGA Nanoparticles: Antioxidant and Anti-microbial Properties.
Odeh, F., Ismail, S.I., Abu-Dahab, R., Mahmoud, I.S., Al Bawab, A., 2012. Thymoquinone in liposomes: a study of loading efficiency and biological activity towards breast cancer. Drug Deliv. 19 (8), 371–377.
Ohkawa, H., Ohishi, N., Yagi, K., 1979. Assay for lipid peroxides in animal tissues by thiobarbituric acid reaction. Anal. Biochem. 95 (2), 351–358.
Oluyemi, K.A., Omotuyi, I.O., Jimoh, O.R., Adesanya, O.A., Saalu, C.L., Josiah, S.J., 2007. Erythropoietic and anti-obesity effects of Garciniacambogia (bitter kola) in Wistar rats. Biotechnol. applied Biochem. 46 (1), 69–72.
Patrick-Iwuanyanwu, K.C., Wegwu, M.O., Ayalogu, E.O., 2007. Prevention of CCl4 induced liver damage by ginger, garlic and vitamin E. Pak. J. Biol. Sci. 10, 617–621.
Sadettin, S., Donmez, G., 2007. Simultaneous bioaccumulation of reactive dye and chromium (VI) by using thermophile Phormidium sp. Enzyme Microb. Technol. 41 (1), 175–180.
Schwabe, R.F., Brenner, D.A., 2006. Mechanisms of liver injury. I. TNF-alpha-induced liver injury: role of IKK, JNK and ROS pathways. Am. J. Physiol. Gastrointest. Liver Physiol. 290, 583–589.
Shah, V., Garg, N., Madamwar, D., 2001. An integrated process of textile dye removal and hydrogen evolution using cyanobacterium, Phormidiumvalderianum. World J. Microbiol. Biotechnol 17 (5), 499–504.
Singh, S.C., Sinha, R.P., Hader, D.P., 2002. Role of lipids and fatty acids in stress tolerance in cyanobacteria. Acta Protozool. 41 (4), 297–308.
Skulberg, O.M., 2000. Microalgae as a source of bioactive molecules–experience from cyanophyte research. J. Appl. Phycol. 12 (3), 341–348.
Syiem, M.B., Bhattacharjee, A., 2010. An efficient protocol for long-term preservation of cyanobacteria. J. Adv. Lab. Res. Biol. 1, 53–59.
Sylvester, B., Porfire, A., Muntean, D.M., Vlase, L., Lupuţ, L., Licarete, E., Sesarman, A., Alupei, M.C., Banciu, M., Achim, M., Tomuţă, I., 2016. Optimization of prednisolone-loaded long-circulating liposomes via application of Quality by Design (QbD) approach. J. Liposome Res. 26, 1–13.
Wang, Y., Tu, S., Li, R., Yang, X., Liu, L., Zhang, Q., 2010. Cholesterol succinyl chitosan anchored liposomes: preparation, characterization, physical stability, and drug release behavior. Nanomed.: Nanotech. Biol. Med. 6 (3), 471–477.
Xu, X., Khan, M.A., Burgess, D.J., 2011. A quality by design (QbD) case study on liposomes containing hydrophilic API: I. Formulation, processing design and risk assessment. Int. J. Pharm. 419, 52–59.
Xu, X., Khan, M.A., Burgess, D.J., 2012. A quality by design (QbD) case study on liposomes containing hydrophilic API: II. Screening of critical variables, and establishment of design space at laboratory scale. Int. J. Pharm. 423 (2), 543–553.
Zamboni, W.C., 2005. Liposomal, nanoparticle, and conjugated formulations of anticancer agents. Clin. Cancer Res. 11, 8230–8234.